

## Structural and Thermodynamic Analysis of the First Mononuclear Aqueous Aluminum Citrate Complex Using DFT Calculations<sup>†</sup>

Antonio Luiz Oliveira de Noronha, Luciana Guimarães, and Hélio Anderson Duarte\*

*Grupo de Pesquisa em Química Inorgânica Teórica – GPQIT, Departamento de Química-ICEx-UFMG, 31.270-901 Belo Horizonte, MG, Brazil*

Received January 13, 2007

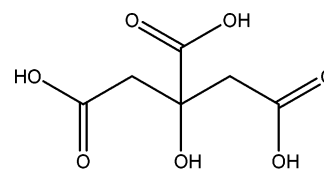
**Abstract:** Structural and thermodynamic properties of the mononuclear Al/citrate complexes have been theoretically investigated aiming to understand the coordination mechanism at an atomic level. GGA-DFT/PCM calculations have been performed for the different conformations and tautomers arising from the  $\text{Al}^{3+}$  and citric acid ( $\text{H}_3\text{L}$ ) interaction in aqueous solution. The Gibbs reaction energies were estimated based on the reaction of the trigonal planar  $\text{Al}(\text{OH})_3$  and  $\text{H}_3\text{L}$  to form different Al–citrate complexes. The estimated Gibbs free reaction energies for the  $[\text{AlL}]$ ,  $[\text{AlHL}]^+$ , and  $[\text{Al}(\text{OH})\text{L}]^-$  species are in good agreement with the experimental values. In these species, the  $\text{Al}^{3+}$  center is coordinated by two carboxylic and the tertiary hydroxyl groups of the citrate. Conversely to what has been proposed based on the experiments, the present theoretical calculations indicate that the citric acid hydroxyl group remains protonated upon the coordination of  $\text{Al}^{3+}$ . In fact, our model turns out to be more consistent with the relative  $\text{p}K_{\text{a}}$  values of citrate protonation groups and with the hydrolysis constant of the  $\text{H}_2\text{O}$  bound to  $\text{Al}^{3+}$  leading to better agreement with the available experimental data.

### Introduction

Aluminum is present in a wide range of areas in every day life and is the major constituent of soil. Aluminum, and its chemical speciation in the presence of different ligands, has attracted a great deal of attention<sup>1–6</sup> due to its importance in many processes related to environment, biology, and materials. The  $\text{Al}(\text{III})$  ion in aqueous solution is a rather complex system<sup>7</sup> due to the formation of many hydrolysis species with different stoichiometries. Furthermore, in the presence of ligands, such as organic acids,  $\text{Al}(\text{III})$  is coordinated forming many different species. The role of these species in the environment and biological processes is still an open question and has deserved a great deal of attention in the past few years.<sup>8–14</sup>

Citrate acid ( $\text{H}_3\text{L}$ )—structure 1—is a very versatile molecule with three carboxylic groups and one tertiary hydroxyl

group which makes this molecule able to coordinate many different metal ions in aqueous solution.



Structure 1

It is an important organic ligand in nature derived from root exudates, decomposing organic matter, and other sources, influencing drastically the hydrolysis of  $\text{Al}^{3+}$  and, consequently, its speciation in the environment.<sup>15</sup> Citric acid is also the main small molecule in the blood plasma able to coordinate the  $\text{Al}^{3+}$ . It has been found to contribute for decreasing the toxicity of metal ions in living organisms<sup>16</sup> probably due to its capacity of coordinating metal ions. The structural and thermodynamic knowledge of Al–citrate complexes has fundamental importance and, therefore, has been the subject of many investigations. Thermodynamic

<sup>†</sup> Dedicated to Professor Dennis R. Salahub on the occasion of his 60th birthday.

\* Corresponding author phone: ++55-31-3499-5748; fax: ++55-31-3499-5700; e-mail: duarte@ufmg.br.

properties as the equilibrium constants of the different Al/citrate species have been studied using potentiometric measurements.<sup>17,18</sup> It has been shown that mononuclear species are predominant in the blood plasma concerning kinetic and thermodynamic points of view. The AIL complex is the predominant species in the 2–4 pH range followed by deprotonation to form  $[\text{Al}(\text{OH})\text{L}]^{-1}$  which predominates in the 4–6 pH range. The citrate ability to form chelates explains the strong complexes formed with  $\text{Al}^{3+}$  ion.

It is expected that the metal ion,  $\text{Al}^{3+}$ , will be coordinated through the stronger electron donor groups, i.e., the citrate carboxylic groups. If only these carboxylic groups are involved in the  $\text{Al}^{3+}$  coordination, 7-member rings will be formed. However, it is well-known that 7-member rings are not favorable due to bond strengths. Therefore, it has been suggested that the citric acid acts as a tridentate ligand involving carboxylic and hydroxyl groups to form more stable 5- or 6-member rings, depending on which carboxylic groups are involved. In fact, X-ray structure determination<sup>19</sup> has shown that the  $\text{Al}^{3+}$  is coordinated through the hydroxyl group in the  $[(\text{NH}_4)_5\{\text{Al}(\text{C}_6\text{H}_4\text{O}_7)_2\} \cdot 2\text{H}_2\text{O}]$  complex. This mechanism seems to be reasonable even though the carboxylic groups are a much stronger electron donor than the hydroxyl group. The citric acid in aqueous solution presents only three  $\text{pK}_{\text{a,s}}$  (3.13, 4.76, 6.40)<sup>20</sup> which are associated with the carboxylic groups. How do we explain that the hydroxyl group is involved in the metal ion coordination? The answer has been shown to be very trivial: the hydroxyl group is deprotonated! However, in aqueous solution, this seems to be contradictory since the hydroxyl group has not been observed to be deprotonated in the aqueous pH range. As a comparison, the *tert*-butyl alcohol  $\text{pK}_{\text{a}}$  is about 19.

Recently, Aquino et al.<sup>21</sup> have performed density functional (DFT) investigation for the aluminum(III)–citrate system. They have calculated many different conformations of AIL complexes. The solvent effect has been taken into account using the polarizable continuum method (PCM). The free energy of the complex formation is not in agreement with the experimental value with an error of more than 40  $\text{kcal} \cdot \text{mol}^{-1}$ . However, in the literature, there are many examples in which complex formation free energies are predicted with reasonable accuracy (less than 6  $\text{kcal/mol}$ ) using the DFT-GGA/PCM approach.<sup>22–31</sup>

The apparent disagreement between the experimental observations and the proposed structures motivated us to revisit the Al/citrate system, focusing in its first mononuclear complex formation. Experimental techniques can provide normally global information on the thermodynamic stability of different species. The goal of this work is to provide a detailed picture of Al/citrate chemical speciation aiming to contribute to the understanding of this complex system at an atomic level.

## Computational Aspects

All possible conformations and tautomers arising from the interaction of  $\text{Al}^{3+}$  with citric acid ( $\text{H}_3\text{L}$ ) were calculated using the LCGTO-KS-DFT method (Linear Combination of Gaussian Type Orbital–Kohn–Sham–Density functional)

implemented in the deMon program.<sup>32</sup> The following exchange correlation (XC) functionals based on the generalized gradient approximation were employed: BP86, with the Becke<sup>33</sup> expression for the exchange and the Perdew<sup>34,35</sup> expression for correlation and the PBE XC functional that employs the expressions developed by Perdew, Burke, and Ernzerhof.<sup>36</sup> The DZVP and TZVP basis sets explicitly optimized for DFT<sup>37</sup> and the Ahlrichs basis sets (A-PVTZ)<sup>38</sup> have been used.

Auxiliary basis sets, automatically generated (A2\*), were used for fitting the charge density. An adaptative grid<sup>39,40</sup> with a tolerance of  $10^{-6}$  was employed in the numerical integrations of the exchange–correlation energy and potential.

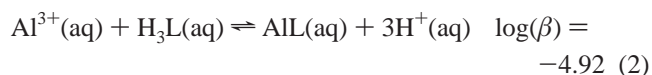
All complexes were fully optimized in the gas phase, without symmetry restrictions using the standard scheme Broyden–Fletcher–Goldfarb–Shanno (BFGS).<sup>41</sup> Harmonic vibrational analyses were performed, and the Hessian matrix was evaluated numerically from the analytical gradients of the potential energy surface (PES). Positive frequencies ensure that a minimum was found in the PES. All geometry optimization and harmonic frequency calculations have been carried out in the gas phase with the deMon program. Thermodynamic properties were obtained following the canonical formalism<sup>42</sup> at 298 K. Nonspecific solvent effects were obtained from the United Atoms Hartree–Fock/Polarizable Continuum model (UAHF/PCM).<sup>43,44</sup> As described by Saracino,<sup>45</sup> in all UAHF/PCM calculations, the cavity radii were obtained by single point calculations at the HF/6-31G(d,p) level, using the DFT optimized geometries. The solvation free energies were obtained using the Gaussian 98 program suite.<sup>46</sup>

It is worth separating the reaction free energy in aqueous solution as the sum of three parts: electronic plus nuclear repulsion energy ( $\Delta E^{\text{ele}}$ ), thermal contribution ( $\Delta G^{\text{T}}$ ), and solvation free energy ( $\Delta G^{\text{solv}}$ ), as given in eq 1. The thermal contribution is estimated using the ideal gas model, the calculated harmonic vibrational frequencies to estimate the zero point energy correction (ZPE), and the correction due to the thermal population of vibrational levels.

$$\Delta G_{\text{aq}}^{\text{tot}} = \Delta E^{\text{ele}} + \Delta G^{\text{T}} + \Delta G^{\text{solv}} \quad (1)$$

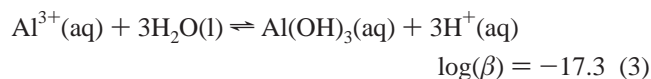
## Results and Discussion

The  $\text{Al}^{3+}$  ion interacts with citric acid ( $\text{H}_3\text{L}$ ) to form species 1:1 and 1:2 metal:ligand proportion. The predominant species in acid solution is the 1:1 species as it has been shown by Öhman.<sup>18</sup> The AIL species formation is usually described from the interaction of  $\text{Al}^{3+}(\text{aq})$  and citric acid ( $\text{H}_3\text{L}$ ) according to eq 2.<sup>18</sup>

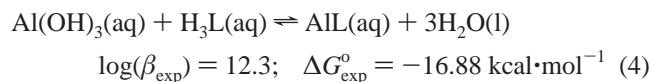


Theoretical estimation of the stability constants of complexes in solution is still a challenging task mostly due to the difficulty in estimating the solvation free energy variation,  $\Delta G^{\text{solv}}$ , term of eq 1. In fact, solvation free energies variation of reactants with neutral charges are better described by the UAHF/PCM approach as it has been shown elsewhere.<sup>26,27,31</sup> On the other hand,  $\text{Al}(\text{OH})_3(\text{aq})$  is

formed according to eq 3.<sup>18</sup>



Therefore it is possible to rewrite eq 2 using eq 3 leading to the reaction equation in which all reactants are neutral, as described by eq 4.



This strategy has been shown to be very useful in order to obtain reaction equations that are more adequate to be described by the DFT/PCM approach.<sup>27,31</sup> Nevertheless, each of the reactants has to be correctly modeled in solution in order to predict the reaction Gibbs free energy of the AIL formation described by eq 4. It is also important to note that the  $\Delta G_{\text{exp}}^{\circ}$ , shown in eq 4, has larger error bars due to error propagation. Furthermore, stability constants of species that are present only in a small amount—as it is the case of the  $\text{Al}(\text{OH})_3$  species—estimated from potentiometric measurements are normally associated with larger error bars.

**$\text{Al}(\text{OH})_3(\text{aq})$ .** The  $\text{Al}(\text{OH})_3(\text{aq})$  species has a trigonal planar geometry as it is expected. However, in solution, one can argue that the best model for this species could be any one of the  $[\text{Al}(\text{OH})_3(\text{H}_2\text{O})]$ ,  $[\text{Al}(\text{OH})_3(\text{H}_2\text{O})_2]$ , and  $[\text{Al}(\text{OH})_3(\text{H}_2\text{O})_3]$  structures. This is reasonable since in solution water molecules can act as ligands in the first solvation shell. Our results showed no tendency for the water molecule to be at the coordination sphere of the aluminum center in the  $\text{Al}(\text{OH})_3$  species. The hexacoordinated species is not a minimum in the potential energy surface, and the water molecules are not bonded to the aluminum. The coordination of one water molecule in  $[\text{Al}(\text{OH})_3]$ , forming tetrahedral  $[\text{Al}(\text{OH})_3(\text{H}_2\text{O})]$ , is not favorable by 3 kcal·mol<sup>-1</sup>. The inclusion of two water molecules, forming  $[\text{Al}(\text{OH})_3(\text{H}_2\text{O})_2]$ , has a Gibbs free energy of about 12 kcal·mol<sup>-1</sup>. A detailed observation of estimated Gibbs free energy shows that the electronic energy,  $\Delta E^{\text{ele}}$ , is favorable for  $[\text{Al}(\text{OH})_3(\text{H}_2\text{O})]$  formation; however, the thermal,  $\Delta G^{\text{T}}$ , and solvation,  $\Delta G^{\text{solv}}$ , contributions are very positive, making the system nonstable. This is coherent once the water molecules become more labile with the rise in temperature and will not participate as a ligand in the first coordination sphere. Actually, Ikeda et al.<sup>47</sup> showed from Car–Parrinello molecular dynamics that the trigonal planar  $\text{Al}(\text{OH})_3$  is formed in solution.

Recently, Rudolph et al.<sup>48</sup> measured the Raman spectra of the aqueous Al(III) and compared it with ab initio calculations at the 6-31+G\*/MP2 level. They suggested that a complete second shell of solvation with 12 water molecules is necessary in order to reproduce the Raman spectra of Al(III) in solution. One could argue that this approach could also be suitable for the  $\text{Al}(\text{OH})_3$  in solution stabilizing water molecules in the first solvation shell. According to Asthagiri et al.,<sup>49</sup> and we concur, this approach lacks a statistical mechanical foundation. The water molecules in the second solvation shell are normally placed maximizing the hydrogen bonds through full geometry optimization. This invariably leads to artifacts which do not represent the average of the

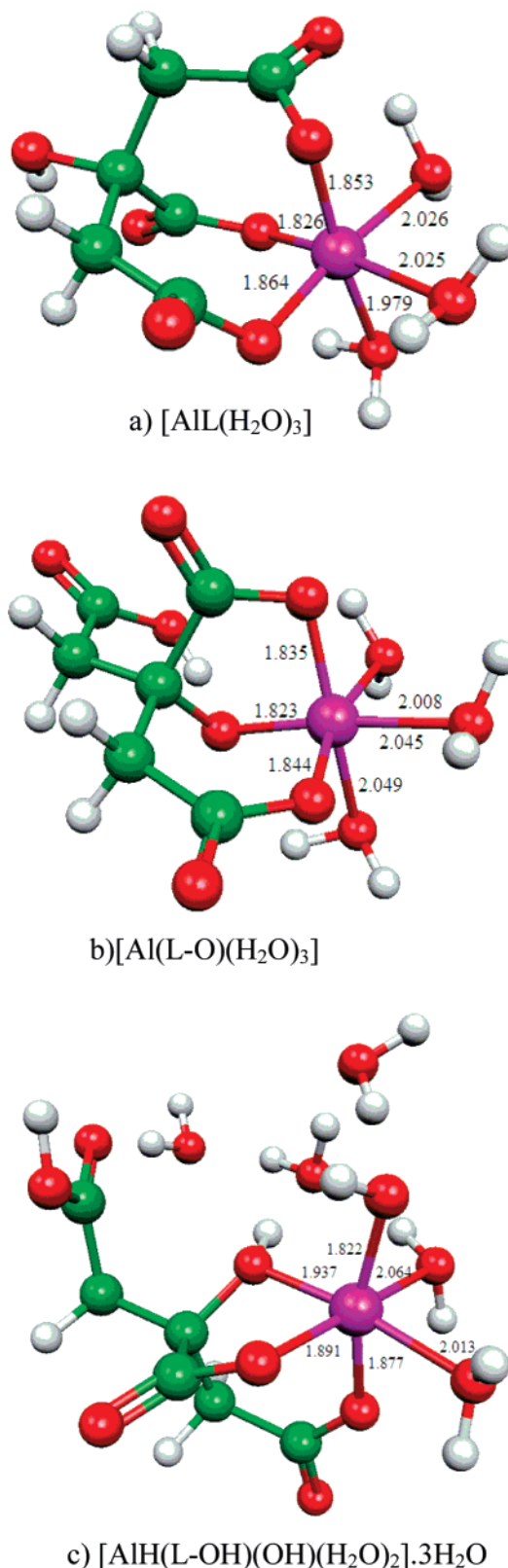


**Figure 1.** PBE/TZVP optimized geometries representative of the AIL complex. Bond distances are in Å.

configurational space of water molecules located in this second solvation shell.

**AIL(aq).** Citric acid has 4 possible donors; however, due to the steric hindrance this molecule can only act as a tridentate ligand. In a 1:1 Al: citrate complex, the coordination number of the metal center still remains to be determined.

**Table 1.** Reaction Free Energies for the Formation of Al(III)/Citrate Species Using Different Levels of Theory<sup>a,b</sup>

reactions	basis sets	$\Delta E^{\text{ele}}$	$\Delta G^{\text{T } c}$	$\Delta G^{\text{solv}}$	$\Delta G^{\text{tot } d}$	$\log(\beta)$
$\text{Al}(\text{OH})_3 + \text{H}_3\text{L} \rightarrow [\text{Al}(\text{L})(\text{H}_2\text{O})_3]$	BP86/DZVP	-38.99	18.72	17.97	-2.30	1.7
	BP86/ A-PVTZ	-38.74			-2.05	1.5
	BP86/TZVP	-36.82			-0.13	0.1
	PBE/DZVP	-42.00			-5.31	3.9
	PBE/ A-PVTZ	-41.62			-4.68	3.4
	PBE/TZVP	-39.12			-2.43	1.8
$\text{Al}(\text{OH})_3 + \text{H}_3\text{L} \rightarrow [\text{Al}(\text{L}-\text{O})(\text{H}_2\text{O})_3]$	BP86/DZVP	-34.32	18.00	10.86	-5.46	4.0
	BP86/ A-PVTZ	-34.26			-5.40	4.0
	BP86/TZVP	-28.57			0.29	-0.2
	PBE/DZVP	-35.88			-7.02	5.1
	PBE/ A-PVTZ	-37.37			-8.51	6.2
	PBE/TZVP	-34.32			-5.46	4.0
$\text{Al}(\text{OH})_3 + \text{H}_3\text{L} + 3\text{H}_2\text{O}^e \rightarrow [\text{AlH}(\text{L}-\text{OH})(\text{OH})(\text{H}_2\text{O})_2] \cdot 3\text{H}_2\text{O}$	BP86/DZVP	-55.81	53.80	-3.23	-12.37	9.1
	BP86/ A-PVTZ	-55.08			-11.60	8.5
	BP86/TZVP	-52.10			-8.66	6.4
	PBE/DZVP	-84.35			-33.79	24.7
	PBE/ A-PVTZ	-62.78			-19.34	14.2
	PBE/TZVP	-57.90			-14.46	10.6
experimental					-16.88	12.3

<sup>a</sup> All energies are in kcal·mol<sup>-1</sup>. <sup>b</sup> Medium used in PCM model is water ( $\epsilon = 78.4$ ). <sup>c</sup> Thermal contribution at 298 K including the zero point energy (ZPE). <sup>d</sup>  $\Delta G^{\text{tot}} = \Delta E^{\text{ele}} + \Delta G^{\text{T}} + \Delta G^{\text{solv}} - nRT \ln[\text{H}_2\text{O}]$ . <sup>e</sup> The presence of water molecules in the reactants are corrected with the expression  $-nRT \ln[\text{H}_2\text{O}]$ , where  $n$  represents the number of water molecules.<sup>28,52</sup>

The water can act as a ligand to fulfill the available coordination sites of  $\text{Al}^{3+}$  in the complex. Citric acid can also coordinate the aluminum ion in different ways. The most favorable complexes with 6- and 5-member rings which bind the  $\text{Al}^{3+}$  through the carboxylic and the hydroxyl groups have been investigated. The 7-member rings formed when the three carboxylic groups are involved in the metal coordination have also been calculated. The available coordination sites of the aluminum center have been fulfilled with water molecules acting as ligands. The tetrahedral and bipyramid structures with one and two water molecules, respectively, are at least 14 kcal·mol<sup>-1</sup> higher in energy than the octahedral species.

Figure 1 shows the optimized geometry structures possible to describe the AIL complex in solution. The first structure (Figure 1a) involves the three acidic carboxylic groups forming 7-member rings. Although with the presence of less favorable 7-member rings, it seems reasonable since the carboxylic groups are much more acidic than the tertiary hydroxyl group of the citrate.

The second structure (Figure 1b) is the one normally proposed as the most reasonable since it has 5- and 6-member rings involving the deprotonated hydroxyl group. In order to keep the neutrality, the acidic carboxylic group that is not coordinating the metal center is protonated. This structure has been proposed based on X-ray evidence that 5- and 6-member rings are formed involving the hydroxyl group.<sup>19</sup> Matzapetakis et al. suggested the formula  $[(\text{NH}_4)_5\{\text{Al}(\text{C}_6\text{H}_4\text{O}_7)_2\} \cdot 2\text{H}_2\text{O}]$  with the citrate fully deprotonated (i.e., the hydroxyl group is also deprotonated). However, analyzing carefully the preparation and the crystal structure one observes that the formula  $[(\text{NH}_4)_3\{\text{Al}(\text{C}_6\text{H}_5\text{O}_7)_2\} \cdot 2\text{NH}_4\text{OH}]$  is also consistent, which would have the citrate hydroxyl group protonated. It is important to note that, according to the authors, the pH was adjusted to 8 with  $\text{NH}_4\text{OH}(\text{aq})$  during the preparation. In aqueous solution, it is unlikely that the

citrate tertiary hydroxyl group will be deprotonated under the coordination with  $\text{Al}^{3+}$  once this group has a  $\text{pK}_a$  of about 19 (*tert*-butyl alcohol). Furthermore, there is a great deal of evidence that the  $-\text{OH}$  group can bridge different centers as it is observed in the gibbsite. Recently, the proposed mechanism for  $\text{As}(\text{OH})_3$  adsorption on the gibbsite involves the  $-\text{OH}$  bridging As/Al centers.<sup>50</sup> Therefore, it is reasonable to propose a structure in which the hydroxyl group remains protonated, and either the free carboxylic group or one of the water molecules bound to  $\text{Al}^{3+}$  center is deprotonated. A zwitterion is formed, with a positive charge on the  $\text{Al}^{3+}$  center and a negative charge on the carboxylic group not involved in the Al center coordination. The zwitterion is formed normally in aqueous solution increasing the dipole moment and enhancing the interaction with the polar solvent. Then, the optimization of this structure at the gas phase leads, invariably, to a nonzwitterionic form, i.e., the hydrogen migrates from the hydroxyl group to the carboxylic group. In order to avoid this migration and stabilize the zwitterionic form, three water molecules were placed around the citrate hydroxyl group. The fully optimized structure is shown in Figure 1c. It is interesting to observe that the free carboxylic group turns out to be protonated due to a proton migration from one of the water molecules bound to the  $\text{Al}^{3+}$  center. This is consistent with the relative  $\text{pK}_a$  of the different groups involved. The first  $[\text{Al}(\text{H}_2\text{O})_6]^{3+}$   $\text{pK}_a$  is about 5.52, and the third citrate  $\text{pK}_a$  is about 6.40, consequently, the structure shown in Figure 1c is reasonable. However, the structure with the free carboxylic group deprotonated cannot be disregarded. Actually, both can be present in the medium, and they cannot be distinguished through potentiometric measurements.

**Gibbs Free Energy Estimate.** The estimated Gibbs free energy of the reaction described by eq 4, leading to different structures of the  $\text{Al}^{3+}$  coordination by citric acid, is shown



in Table 1. The reaction free energy has been separated in each contribution according to eq 1.

The estimate of equilibrium constants of reactions in a condensed medium is a very difficult task. It has been pointed out by De Abreu et al.<sup>25</sup> that the DFT calculated thermal contribution is insensitive to the choice of the XC functional and basis sets. They showed that the difference is not larger than 1 kcal·mol<sup>-1</sup>. Therefore, we decided to calculate this contribution at the level of BP86/DZVP. The UAHF/PCM method has limitations as with any other method based on the continuum models for estimating solvation energy. Specific interaction of the solvent with the solute is not taken into account in this type of model. However, in the literature, there is enough evidence that these specific interactions are canceled when the reaction involves similar reactants and products.<sup>24,45,51</sup> It has been speculated that a great part of the success of estimating equilibrium constant values is due to a good synergism between the level of theory, basis sets, and the continuum method leading to error compensation.<sup>25</sup>

According to Table 1, [AlH(L-OH)(OH)(H<sub>2</sub>O)<sub>2</sub>] is the most favorable species. Other structures investigated are at least 6 kcal·mol<sup>-1</sup> higher in energy. The favorable solvation energy observed for the reaction forming [AlH(L-OH)(OH)(H<sub>2</sub>O)<sub>2</sub>] (Figure 1c) is a consequence of the charge separation in the structure enhancing the solvation. The Gibbs free energy of this reaction (eq 4) is -14.46 kcal·mol<sup>-1</sup> at the PBE/TZVP/PCM level of theory, only 2.42 kcal·mol<sup>-1</sup> larger than the experimental value. The scheme PBE/TZVP/PCM has been shown to provide pK<sub>a</sub> values and hydrolysis constants for Fe<sup>3+</sup> and Fe<sup>2+</sup> in good agreement with experimental values.<sup>28,29</sup> The error bars are about 4 kcal·mol<sup>-1</sup> which is reasonable if one takes into account that the ionic strength of the solution is neglected and the error bars of the experimental free energies quoted from experimental equilibrium constants are normally about 1 logarithmic unit, that is, about 1.4 kcal·mol<sup>-1</sup>. These results support the [AlH(L-OH)(OH)(H<sub>2</sub>O)<sub>2</sub>] model for the AIL complex in which the hydroxyl group remains protonated, while one water molecule bound to the Al<sup>3+</sup> center is hydrolyzed. This is in agreement with the relative pK<sub>a</sub> of the different groups present in citric acid, the first [Al(H<sub>2</sub>O)<sub>6</sub>]<sup>3+</sup> pK<sub>a</sub>, and with the perception that 5- and 6-membered rings are more stable.

One could argue that other 1:1 Al/citrate complexes have been observed from potentiometric experiments and that they are derived from this neutral AIL species. Actually, two species are observed: [AlHL]<sup>+</sup> and [Al(OH)L]<sup>-</sup>.<sup>18</sup> The protonated species probably has its carboxylic group protonated, and only water molecules occupy the available coordination sites of the Al<sup>3+</sup> center since this species is predominant in a pH less than 3. The [Al(OH)L]<sup>-</sup> predominates in pH above 4, and, consequently, the citrate free carboxylic group should be deprotonated. This is consistent with the third pK<sub>a</sub> of citric acid which is about 6.4. In order to verify if these models are adequate to describe these species in solution, we have estimated the formation constants of these two species using, as a starting point, the neutral [AlH(L-OH)(OH)(H<sub>2</sub>O)<sub>2</sub>] species. Figure 2 shows the optimized structures of [AlH(L-OH)(H<sub>2</sub>O)<sub>3</sub>]<sup>+</sup> and [Al(L-OH)(OH)(H<sub>2</sub>O)<sub>2</sub>]<sup>-</sup> species. The Gibbs free energy of the [AlH-

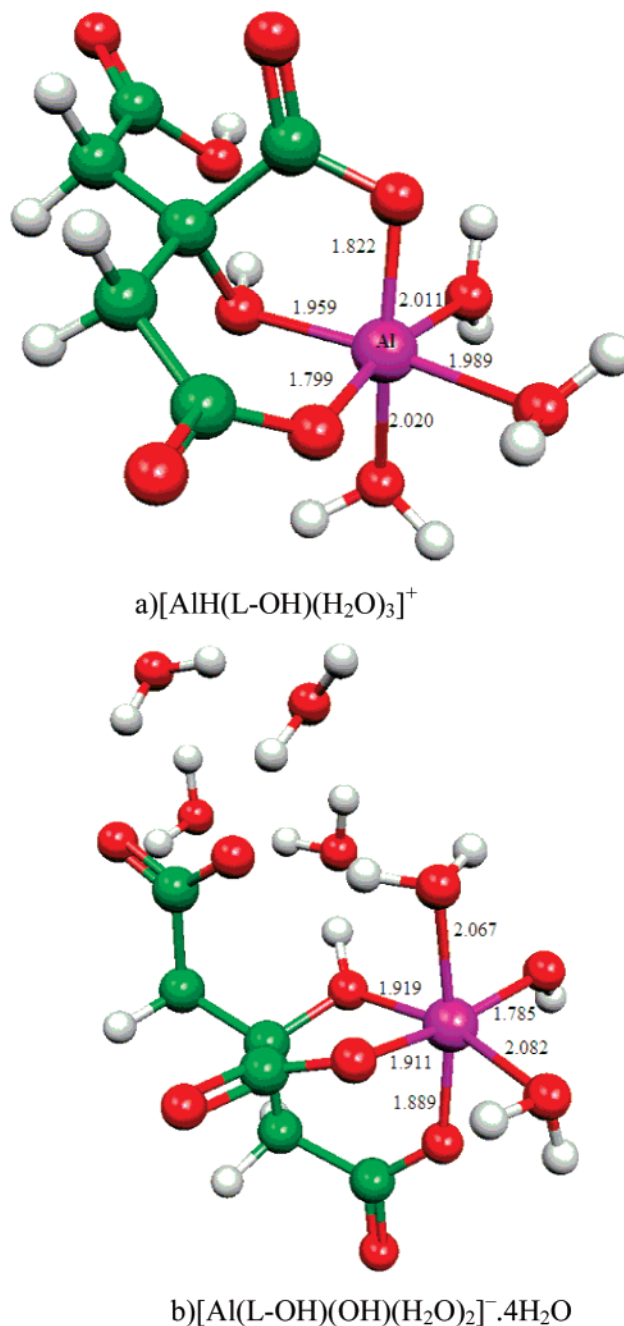


**Figure 2.** PBE/TZVP optimized structures of the protonated and deprotonated [Al(L-OH)(H<sub>3</sub>O)<sub>3</sub>] complex. Bond distances are in Å.

(L-OH)(H<sub>2</sub>O)<sub>3</sub>]<sup>+</sup> formation is in very good agreement with the available experimental data, with an error of only 1.1 and 1.6 kcal·mol<sup>-1</sup> at the PBE/TZVP/PCM and PB86/TZVP/PCM levels of theory, respectively. The positive charged complexes are usually well described by the continuum model which impact the final results. The [AlH(L-OH)(H<sub>2</sub>O)<sub>3</sub>]<sup>+</sup> optimized structure is shown in Figure 2a. The Al-OH<sub>2</sub> bond distances are about 2.0 Å, and the Al-O(carbonyl) is about 1.8 Å. The predicted Al-O(hydroxyl) distance is 1.959 Å which is close to the observed value of 1.937 Å for the [AlH(L-OH)(OH)(H<sub>2</sub>O)<sub>2</sub>] complex. For the [Al(L-OH)(OH)(H<sub>2</sub>O)<sub>2</sub>]<sup>-</sup> species, the Gibbs free energy is about -21.46 and -14.71 kcal·mol<sup>-1</sup> at PBE/TZVP/PCM and PB86/TZVP/PCM, respectively. These values must be compared

**Table 2.** Reaction Free Energies for the Formation of Al(III)/Citrate Charged Species Using Different Levels of Theory<sup>a,b,e</sup>

reaction	basis set	$\Delta G^{\text{ele}}$	$\Delta G^{\text{Tc}}$	$\Delta G^{\text{solv}}$	$\Delta G^{\text{tot d}}$	$\log(\beta)$
Al(OH) <sub>3</sub> + H <sub>3</sub> L + H <sub>3</sub> O <sup>+</sup> → [Al(L-OH)(H <sub>2</sub> O) <sub>3</sub> ] <sup>+</sup> + H <sub>2</sub> O	BP86/DZVP	-85.91	2.26	59.10	-22.17	16.3
	BP86/A-PVTZ	-85.88			-22.14	16.2
	BP86/TZVP	-85.20			-21.46	15.7
	PBE/DZVP	-88.62			-24.88	18.2
	PBE/A-PVTZ	-88.55			-24.81	18.2
	PBE/TZVP	-84.70			-20.96	15.4
experimental					-19.90	14.6
Al(OH) <sub>3</sub> + H <sub>3</sub> L + 4H <sub>2</sub> O → [Al(L-OH)(OH)(H <sub>2</sub> O) <sub>2</sub> ] <sup>-</sup> ·3H <sub>2</sub> O + H <sub>3</sub> O <sup>+</sup>	BP86/DZVP	50.61	65.74	-135.32	-21.35	15.7
	BP86/A-PVTZ	47.23			-24.73	18.1
	BP86/TZVP	57.25			-14.71	10.8
	PBE/DZVP	42.80			-29.16	21.4
	PBE/A-PVTZ	38.30			-33.66	24.7
	PBE/TZVP	50.50			-21.46	15.7
experimental					-12.0	8.8

<sup>a</sup> All energies are in kcal·mol<sup>-1</sup>. <sup>b</sup> Medium used in PCM model is water ( $\epsilon = 78.4$ ). <sup>c</sup> Thermal contribution at 298 K, calculated at the BP86/DZVP level. <sup>d</sup>  $\Delta G^{\text{tot}} = \Delta E^{\text{ele}} + \Delta G^{\text{T}} + \Delta G^{\text{solv}} - \pm nRT \ln[\text{H}_2\text{O}]$ . <sup>e</sup> The presence of water molecules in the reactants or products are corrected with the expression  $\pm nRT \ln[\text{H}_2\text{O}]$ , where  $n$  represents the number of water molecules.<sup>28,52</sup>

with the experimental estimated value of  $-12.00 \text{ kcal}\cdot\text{mol}^{-1}$ . The larger errors (about 9 and 3 kcal·mol<sup>-1</sup> for PBE/TZVP/PCM and BP86/TZVP/PCM, respectively) are due to the difficulty in treating negatively charged complexes. The free solvation energy of negative charged systems is difficult to estimate through the PCM model. Furthermore, the electronic energy is more sensitive to basis set quality since more diffuse basis functions are necessary to treat anions adequately. These limitations will impact the total free energy of the reaction. However, it is possible to see from Table 2 that the observed trends are consistent. In general the PBE/TZVP/PCM method provides total free energies in better agreement with available experimental data. The exception is the negatively charged species for which the BP86/TZVP/PCM predicted value is in better agreement with the experimental data. The [Al(L-OH)(OH)(H<sub>2</sub>O)<sub>2</sub>]<sup>-</sup> optimized structure is shown in Figure 2b. The Al-O(hydroxyl) distance is about 1.919 Å, and it did not change very much with the deprotonation of the species. The Al-OH<sub>2</sub> bond distances are also about 2.07 Å, as expected. The Al-OH bond distance is about 1.785 Å.

Even though equilibrium constant estimates in aqueous solution are still challenging for theoretical chemistry, insights about the chemical speciation mechanism have been provided for several complexes systems based on DFT calculations and continuum methods with remarkable success.<sup>22-25,27-29</sup> In the present work, the Gibbs free energies of the Al<sup>3+</sup> coordination by citric acid forming mononuclear complexes in aqueous solution have been estimated. Conversely to what has been proposed based on the experiments, the present theoretical calculations predict that the citric acid hydroxyl group is not deprotonated even when it is involved in the coordination of the Al<sup>3+</sup>. This is consistent with the relative citric acid pK<sub>a</sub> values and the Al<sup>3+</sup> hydrolysis constant. Other 1:1 Al/citrate complexes with a different degree of protonation have also been calculated, and the reaction free energies have been estimated. The model in which the hydroxyl group remains protonated while involved in the coordination of the metal center leads to a better agreement with the available experimental data.

## Final Remarks

The Al<sup>3+</sup> hydrolysis is already a complex system with many hydroxylated species.<sup>7</sup> In the presence of citric acid, stable and metastable complexes are formed, and mononuclear complexes at low citrate concentrations are predominant.<sup>18</sup> It has been suggested that the citrate ligand is completely deprotonated including its tertiary hydroxyl group.<sup>19</sup> In our point of view, this is not consistent with acidic properties of this molecule and the Al<sup>3+</sup> in solution. The hydroxyl group deprotonation is only possible at very high pH or in stringent conditions. However, the hydroxyl group has been unambiguously proven to be involved in the coordination of Al<sup>3+</sup>. Our results indicate the hydroxyl group remains protonated while coordinating the Al<sup>3+</sup> center. This model is coherent with the potentiometric measurements since the degree of protonation of the species is not changed. In fact, the calculations indicate that the citrate carboxylic group and the H<sub>2</sub>O bound to Al<sup>3+</sup> are more acidic than the citrate -OH group, as it is expected. This might have important consequences in understanding the chemical speciation of the Al<sup>3+</sup>/citrate system at high pH when polynuclear species are present.

**Acknowledgment.** We would like to thank the following Brazilian Research Agencies for support: Conselho Nacional para o Desenvolvimento Científico e Tecnológico (CNPq), Coordenação de Aperfeiçoamento de Pessoal de Ensino Superior (CAPES), and Fundação de Amparo à Pesquisa do Estado de Minas Gerais (FAPEMIG). The PRONEX-FAPEMIG (EDT 2403/03) is also gratefully acknowledged.

## References

- (1) Huh, J. W.; Choi, M. M.; Lee, J. H.; Yang, S. J.; Kim, M. J.; Choi, J.; Lee, K. H.; Lee, J. E.; Cho, S. W. Activation of monoamine oxidase isotypes by prolonged intake of aluminum in rat brain. *J. Inorg. Biochem.* **2005**, *99*, 2088–2091.
- (2) Zhang, F. P.; Ji, M.; Xu, Q.; Yang, L.; Bi, S. P. Linear scan voltammetric indirect determination of Al-III by the catalytic cathodic response of norepinephrine at the hanging mercury drop electrode. *J. Inorg. Biochem.* **2005**, *99*, 1756–1761.

- (3) Esteves, M. A.; Cachudo, A.; Chaves, S.; Santos, M. A. New silica-immobilized hydroxypyrimidinone as sorbent of hard metal ions from aqueous fluids. *J. Inorg. Biochem.* **2005**, *99*, 1762–1768.
- (4) Drabek, O.; Mladkova, L.; Boruvka, L.; Szakova, J.; Nikodem, A.; Nemecek, K. Comparison of water-soluble and exchangeable forms of Al in acid forest soils. *J. Inorg. Biochem.* **2005**, *99*, 1788–1795.
- (5) Boruvka, L.; Mladkova, L.; Drabek, O. Factors controlling spatial distribution of soil acidification and Al forms in forest soils. *J. Inorg. Biochem.* **2005**, *99*, 1796–1806.
- (6) Missel, J. R.; Schetinger, M. R.; Gioda, C. R.; Bohrer, D. N.; Pacholski, I. L.; Zanatta, N.; Martins, M. A.; Bonacorso, H.; Morsch, V. M. Chelating effect of novel pyrimidines in a model of aluminum intoxication. *J. Inorg. Biochem.* **2005**, *99*, 1853–1857.
- (7) Casey, W. H. Large aqueous aluminum hydroxide molecules. *Chem. Rev.* **2006**, *106*, 1–16.
- (8) Pokrovsky, O. S.; Dupre, B.; Schott, J. Fe-Al-organic colloids control of trace elements in peat soil solutions: Results of ultrafiltration and dialysis. *Aquat. Geochem.* **2005**, *11*, 241–278.
- (9) Jelic, R. M.; Joksovic, L. G.; Djurdjevic, P. T. Potentiometric study of the effect of sodium dodecylsulfate and dioxane on the hydrolysis of the aluminum(III) ion. *J. Solution Chem.* **2005**, *34*, 1235–1261.
- (10) Swaddle, T. W.; Rosenqvist, J.; Yu, P.; Bylaska, E.; Phillips, B. L.; Casey, W. H. Kinetic evidence for five-coordination in  $\text{AlOH}(\text{aq})(2+)$  ion. *Science* **2005**, *308*, 1450–1453.
- (11) Hiradate, S. Speciation of aluminum in soil environments. *Soil Sci. Plant Nutr.* **2004**, *50*, 303–314.
- (12) Lakatos, A.; Bertani, R.; Kiss, T.; Venzo, A.; Casarin, M.; Benetollo, F.; Ganis, P.; Favretto, D. Al-III ion complexes of saccharic acid and mucic acid: A solution and solid-state study. *Chem.-Eur. J.* **2004**, *10*, 1281–1290.
- (13) Phillips, B. L.; Lee, A.; Casey, W. H. Rates of oxygen exchange between the  $\text{Al}_2\text{O}_8\text{Al}_{28}(\text{OH})(56)(\text{H}_2\text{O})(26)(18+)$  (aq) (Al-30) molecule and aqueous solution. *Geochim. Cosmochim. Acta* **2003**, *67*, 2725–2733.
- (14) Silwood, C. J. L.; Grootveld, M. Evaluation of the speciation status of aluminium(III) ions in isolated osteoarthritic knee-joint synovial fluid. *Biochim. Biophys. Acta* **2005**, *1725*, 327–339.
- (15) Kuan, W. H.; Wang, M. K.; Huang, P. M.; Wu, C. W.; Chang, C. M.; Wang, S. L. Effect of citric acid on aluminum hydrolytic speciation. *Water Res.* **2005**, *39*, 3457–3466.
- (16) Driscoll, C. T.; Baker, J. P.; Bisogni, J. J.; Schofield, C. L. Effect Of Aluminum Speciation On Fish In Dilute Acidified Waters. *Nature* **1980**, *284*, 161–164.
- (17) Ohman, L. O.; Sjoberg, S. Equilibrium And Structural Studies Of Silicon(Iv) And Aluminum(Iii) In Aqueous-Solution. 9. A Potentiometric Study Of Mono-Nuclear And Poly-Nuclear Aluminum(Iii) Citrates. *J. Chem. Soc., Dalton Trans.* **1983**, 2513–2517.
- (18) Ohman, L. O. Equilibrium And Structural Studies Of Silicon-(Iv) And Aluminum(Iii) In Aqueous-Solution. 17. Stable And Metastable Complexes In The System  $\text{H}^+ - \text{Al}^{3+} - \text{Citric Acid}$ . *Inorg. Chem.* **1988**, *27*, 2565–2570.
- (19) Matzapetakis, M.; Raptopoulou, C. P.; Terzis, A.; Lakatos, A.; Kiss, T. Salifoglou, A. Synthesis, structural characterization, and solution behavior of the first mononuclear, aqueous aluminum citrate complex. *Inorg. Chem.* **1999**, *38*, 618–619.
- (20) Lide, D. R. In *Handbook of Chemical and Physics*; CRC Press: New York, 2004; Vol. 1, Chapter 8, pp 8–50.
- (21) Aquino, A. J. A.; Tunega, D.; Haberhauer, G.; Gerzabek, M. H.; Lischka, H. A density-functional investigation of aluminium(III)-citrate complexes. *Phys. Chem. Chem. Phys.* **2001**, *3*, 1979–1985.
- (22) Li, J.; Fisher, C. L.; Chen, J. L.; Bashford, D.; Noodleman, L. Calculation of redox potentials and  $\text{pK}(\text{a})$  values of hydrated transition metal cations by a combined density functional and continuum dielectric theory. *Inorg. Chem.* **1996**, *35*, 4694–4702.
- (23) Liptak, M. D.; Gross, K. C.; Seybold, P. G.; Feldgus, S.; Shields, G. C. Absolute  $\text{pK}(\text{a})$  determinations for substituted phenols. *J. Am. Chem. Soc.* **2002**, *124*, 6421–6427.
- (24) Liptak, M. D.; Shields, G. C. Accurate  $\text{pK}(\text{a})$  calculations for carboxylic acids using Complete Basis Set and Gaussian-n models combined with CPCM continuum solvation methods. *J. Am. Chem. Soc.* **2001**, *123*, 7314–7319.
- (25) De Abreu, H. A.; De Almeida, W. B.; Duarte, H. A.  $\text{pK}(\text{a})$  calculation of poliprotic acid: histamine. *Chem. Phys. Lett.* **2004**, *383*, 47–52.
- (26) de Noronha, A. L. O.; Duarte, H. A. DFT study of the V(IV)/V(V) oxidation mechanism in the presence of N-hydroxyacetamide. *J. Inorg. Biochem.* **2005**, *99*, 1708–1716.
- (27) Duarte, H. A.; Paniago, E. B.; Carvalho, S.; De Almeida, W. B. Interaction of N-hydroxyacetamide with vanadate: A density functional study. *J. Inorg. Biochem.* **1998**, *72*, 71–77.
- (28) De Abreu, H. A.; Guimaraes, L.; Duarte, H. A. Density-functional theory study of iron(III) hydrolysis in aqueous solution. *J. Phys. Chem. A* **2006**, *110*, 7713–7718.
- (29) Guimaraes, L.; De Abreu, H. A.; Duarte, H. A. Fe(II) hydrolysis in aqueous solution: A DFT Study. *Chem. Phys.* **2007**, *333*, 10–17.
- (30) Kubicki, J. D. Self-consistent reaction field calculations of aqueous  $\text{Al}^{3+}$ ,  $\text{Fe}^{3+}$ , and  $\text{Si}^{4+}$ : Calculated aqueous-phase deprotonation energies correlated with experimental  $\ln(K_{\text{a}})$  and  $\text{pK}(\text{a})$ . *J. Phys. Chem. A* **2001**, *105*, 8756–8762.
- (31) Santos, J. M. D.; Carvalho, S.; Panjago, E. B.; Duarte, H. A. Potentiometric, spectrophotometric and density functional study of the interaction of N-hydroxyacetamide with oxovanadium(IV): the influence of ligand to the V(IV)/V(V) oxi-reduction reaction. *J. Inorg. Biochem.* **2003**, *95*, 14–24.
- (32) Koester, A. M.; Flores, R.; Geudtner, G.; Goursot, A.; Heine, T.; Patchkovskii, S.; Reveles, J. U.; Vela, A.; Salahub, D. *Program deMon 2004-Version 1.1.0 exp*; Aug 2004, Ottawa, Canada, 2004.
- (33) Becke, A. D. Completely Numerical-Calculations On Diatomic-Molecules In The Local-Density Approximation. *Phys. Rev. A* **1986**, *33*, 2786–2788.
- (34) Perdew, J. P. Density-Functional Approximation For The Correlation-Energy Of The Inhomogeneous Electron-Gas. *Phys. Rev. B* **1986**, *33*, 8822–8824.



- (35) Perdew, J. P.; Yue, W. Accurate And Simple Density Functional For The Electronic Exchange Energy-Generalized Gradient Approximation. *Phys. Rev. B* **1986**, *33*, 8800–8802.
- (36) Perdew, J. P.; Burke, K.; Ernzerhof, M. Generalized gradient approximation made simple. *Phys. Rev. Lett.* **1996**, *77*, 3865–3868.
- (37) Godbout, N.; Salahub, D. R.; Andzelm, J.; Wimmer, E. Optimization Of Gaussian-Type Basis-Sets For Local Spin-Density Functional Calculations. I. Boron Through Neon, Optimization Technique And Validation. *Can. J. Chem.* **1992**, *70*, 560–571.
- (38) Schafer, A.; Horn, H.; Ahlrichs, R. Fully Optimized Contracted Gaussian-Basis Sets For Atoms Li To Kr. *J. Chem. Phys.* **1992**, *97*, 2571–2577.
- (39) Krack, M.; Koster, A. M. An adaptive numerical integrator for molecular integrals. *J. Chem. Phys.* **1998**, *108*, 3226–3234.
- (40) Koester, A. M.; Flores-Moreno, R.; Reveles, J. U. Efficient and reliable numerical integration of exchange-correlation energies and potentials. *J. Chem. Phys.* **2004**, *121*, 681–690.
- (41) Schlegel, H. B. Optimization of Equilibrium Geometries and Transition Structures. In *Ab Initio Methods in Quantum Chemistry-I: Advances in Chemical Physics*; Lawley, K. P., Ed.; Wiley: New York, 1987; Vol. 67, pp 249–286.
- (42) McQuarrie, D. A. In *Statistical Thermodynamics*; University Science Books: CA, 1973; Vol. 1, Chapter 8, pp 129–141.
- (43) Cossi, M.; Barone, V.; Cammi, R.; Tomasi, J. Ab initio study of solvated molecules: A new implementation of the polarizable continuum model. *Chem. Phys. Lett.* **1996**, *255*, 327–335.
- (44) Tomasi, J.; Persico, M. Molecular-Interactions In Solution-An Overview Of Methods Based On Continuous Distributions Of The Solvent. *Chem. Rev.* **1994**, *94*, 2027–2094.
- (45) Saracino, G. A. A.; Improta, R.; Barone, V. Absolute pK(a) determination for carboxylic acids using density functional theory and the polarizable continuum model. *Chem. Phys. Lett.* **2003**, *373*, 411–415.
- (46) Frisch, M. J.; Trucks, G. W.; Schlegel, H. B.; Scuseria, G. E.; Robb, M. A.; Cheeseman, J. R.; Zakrzewski, V. G.; Montgomery, J.; Stratmann, R. E.; Burant, J. C.; Dapprich, S.; Millam, J. M.; Daniels, A. D.; Kudin, K. N.; Strain, M. C.; Farkar, O.; Tomasi, J.; Barone, V.; Cossi, M.; Cammi, R.; Mennucci, B.; Pomelli, C.; Adamo, C.; Clifford, S.; Ochterski, J.; Petersson, G. A.; Ayala, P. Y.; Cui, Q.; Morokuma, K.; Malick, D. K.; Rabuck, A. D.; Raghavachari, K.; Foresman, J. B.; Cioslowski, J.; Ortiz, J. V.; Stefanov, B. B.; Liu, G.; Liashenko, A.; Piskorz, P.; Komaromi, I.; Gomperts, R.; Martin, R. L.; Fox, D. J.; Keith, T.; Al-Laham, M. A.; Peng, C. Y.; Nanayakkara, A.; Gonzalez, C.; Challacombe, M.; Gill, P. M. W.; Johnson, B.; Chen, W.; Wong, M. W.; Andres, J. L.; Gonzalez, C.; Head-Gordon, M.; Replogle, E. S.; Pople, J. A. *Gaussian 98, Revision A.6*; Pittsburgh, PA, 1998.
- (47) Ikeda, T.; Hirata, M.; Kimura, T. Hydrolysis of Al<sup>3+</sup> from constrained molecular dynamics. *J. Chem. Phys.* **2006**, *124*, in press.
- (48) Rudolph, W. W.; Mason, R.; Pye, C. C. Aluminium(III) hydration in aqueous solution. A Raman spectroscopic investigation and an ab initio molecular orbital study of aluminium(III) water clusters. *Phys. Chem. Chem. Phys.* **2000**, *2*, 5030–5040.
- (49) Asthagiri, D.; Pratt, L. R.; Paulaitis, M. E.; Rempe, S. B. Hydration structure and free energy of biomolecularly specific aqueous dications, including Zn<sup>2+</sup> and first transition row metals. *J. Am. Chem. Soc.* **2004**, *126*, 1285–1289.
- (50) Oliveira, A. F.; Ladeira, A. C. Q.; Ciminelli, V. S. T.; Heine, T.; Duarte, H. A. Structural model of arsenic(III) adsorbed on gibbsite based on DFT calculations. *J. Mol. Struct. (Theochem)* **2006**, *762*, 17–23.
- (51) Toth, A. M.; Liptak, M. D.; Phillips, D. L.; Shields, G. C. Accurate relative pK(a) calculations for carboxylic acids using complete basis set and Gaussian-n models combined with continuum solvation methods. *J. Chem. Phys.* **2001**, *114*, 4595–4606.
- (52) Pliego, J. R. Thermodynamic cycles and the calculation of pK(a). *Chem. Phys. Lett.* **2003**, *367*, 145–149.

CT700016F